Comparison of Brownian Dynamics Simulations with Microscopic and Light-Scattering Measurements of Polymer Deformation under Flow

Lei Li and Ronald G. Larson*

Department of Chemical Engineering, University of Michigan, Ann Arbor, Michigan 48109

Received July 7, 1999; Revised Manuscript Received December 6, 1999

ABSTRACT: Using Brownian dynamics simulations, we predict the deformation of a polymer coil in dilute solution and compare the results to direct measurements for DNA molecules and for polystyrene. For DNA, optical microscopy measurements of Smith and Chu yield measurements of $\langle x \rangle$, the average projected length of the molecule onto the flow direction as a function of shear rate, while for dilute polystyrene solutions, light scattering experiments yield $\langle R_g^2 \rangle^{1/2}$, the root-mean-square radius of gyration. Both measurements of deformation, $\langle x \rangle$ and $\langle R_g^2 \rangle^{1/2}$, are obtained from the simulations using input parameters required to match the molecular characteristics of both the DNA and the polystyrene solutions used in the experiments. We find that while the agreement between the simulations and the measurements of coil deformation for DNA is excellent, for polystyrene the measured deformation is much less than predicted.

1. Introduction

Since standard rheological measurements do not directly measure polymer size or shape during flow of dilute polymer solutions, light-scattering techniques have been deployed for this purpose. These difficult experiments have been carried out on conventional polystyrene and polyisobutylene solutions both in extensional flow[2−4] and in shear.[5−8] Analogous neutron-scattering experiments have also been conducted in shear.[9] In every case, for both shear and extension, these experiments have yielded apparent polymer flow-induced coil deformations that are far below the predictions of conventional models. These experiments, then, suggest that our understanding of polymer flow-induced deformation might be seriously flawed.

Very recently, however, Chu and his group at Stanford University have developed methods of observing directly the flow-induced deformation of single very large, fluorescently stained, DNA molecules.[1] The measured DNA deformations in both extensional and shear flows are remarkably consistent with predictions of Brownian dynamics simulations of model bead−spring or bead−rod chains.[10,11] In addition, such simulations, and simpler numerical solutions for finitely extensible dumbbell models, provide predictions of extensional viscosities that are in reasonable qualitative agreement with measured viscosities for "Boger fluids"—dilute polymer solutions in viscous solvents.[12,13]

Thus, various comparisons of theoretical predictions with experimental measurements of polymer coil dimensions in flow give a conflicting picture of the degree to which theory and experiment agree. Pinning down experimentally the source of the conflict is complicated by differences from one system to the other in the quantity that is measured. For DNA, the average molecular "stretch" $\langle x \rangle$ is measured, where x is the projection of the molecule onto the flow direction, while for conventional polystyrene or polyisobutylene, light scattering or neutron scattering yields a measurement of the "expansion ratio" of deformed to the undeformed root-mean-square radius of gyration, $e \equiv \langle R_g^2 \rangle_\beta^{1/2} / \langle R_g^2 \rangle_0^{1/2}$. Here the brackets "$\langle\ \rangle$" denote an ensemble-averaged quantity, and the subscript "0" designates the no-flow limit. Not only are different quantities measured, but the theories to which these quantities $\langle x \rangle$ and e have been compared are also different, with e from synthetic polymers being compared to simple dumbbell, Rouse, and Zimm models, while $\langle x \rangle$ for DNA is compared to more sophisticated Brownian dynamics simulations of bead−spring or bead−rod chains with nonlinear elastic properties.

Here, we seek to clarify matters by carrying out Brownian dynamics simulations of DNA and polystyrene dilute solutions in which we compute *both* $\langle x \rangle$ and e. In so doing, we provide a basis by which the differing types of experimental data for these systems can be compared, if not with each other, then at least with a common theoretical model. In an extensional flow, the strain imposed on molecules probed in any real experiment is limited, while in shear arbitrarily large strains can be imposed. Therefore, in a shearing flow we can be confident that the experimental results represent the true steady-state, large-strain limit, while in extension there remain some questions about this point. Hence, we will limit our study to shearing flows, although the implications of the work will also apply to extensional flow.

2. Simulation Method

2.1. Bead−Spring Model. The bead−spring model represents the polymer molecule as a string of N beads and $N - 1$ springs. We compute properties of this model by a standard Brownian dynamics method, with hydrodynamic interactions neglected, as described in our previous paper.[12] As before, for polystyrene, we use for the elastic spring force F_i^{sp} Cohen's Padé approximation[14] to the inverse Langevin (IL) function, which is

$$F_i^{sp} = \frac{k_B T}{b_K} \lambda_i \frac{3 - \lambda_i^2}{1 - \lambda_i^2} \tag{1}$$

10.1021/ma991090z CCC: $19.00
Published on Web 01/26/2000

where λ_i is the extension ratio in spring i

$$\lambda_i = \frac{R_i}{N_{K,s} b_K} \tag{2}$$

Here R_i is the extension of spring i,

$$R_i \equiv |\mathbf{r}_{i+1} - \mathbf{r}_i|; \quad \mathbf{R}_i \equiv \mathbf{r}_{i+1} - \mathbf{r}_i \tag{3}$$

b_K is the Kuhn step length of the freely jointed chain, and $N_{K,s}$ is the number of Kuhn steps per spring. Thus, $L_s = N_{K,s} b_K$ is the fully extended length of a spring. For DNA, we use the wormlike (WL) chain model,[15,16] for which

$$F_i^{sp} = \frac{k_B T}{b_K}\left(\frac{1}{4}(1-\lambda_i)^{-2} - \frac{1}{4} + \lambda_i\right) \tag{4}$$

The definition of the polymer's radius of gyration tensor is

$$\boldsymbol{G} \equiv \frac{1}{2} N^{-2}\left[\sum_{i=1}^{N}\sum_{j=1}^{N} \mathbf{R}_{ij}\mathbf{R}_{ij}\right] \tag{5}$$

where $\mathbf{R}_{ij}$ is the end-to-end vector between monomers i and j, which are bead i and bead j in our model; N is the monomer (bead) number. The radius of gyration squared, R_g^2, is then the trace of the tensor $\boldsymbol{G}$; that is,

$$R_g^2 = \frac{1}{2} N^{-2}\left[\sum_{i=1}^{N}\sum_{j=1}^{N} R_{ij}^2\right] \tag{6}$$

where R_{ij} is the spatial distance between bead i and bead j.

The orientation angle χ in shear is calculated from

$$\chi = \frac{1}{2}\tan^{-1}\left(\frac{2\langle G_{12}\rangle}{\langle G_{11}\rangle - \langle G_{22}\rangle}\right) \tag{7}$$

Here G_{11}, G_{22}, and G_{12} are elements of the radius of gyration tensor $\boldsymbol{G}$, where "1" is the flow direction and "2" the shearing gradient direction.

In the simulations, we also calculate $\langle x\rangle$, the average of the molecule's projected length in the flow direction, so that we can compare the simulation results with the DNA experimental results.

To calculate the dimensionless shear rate, $\beta \equiv \dot{\gamma}\tau$, we calculate the sum of relaxation times from the Rouse model, which is

$$\tau = \sum_{i=1}^{N} \tau_i \approx \frac{\pi^2}{6}\tau_1 \tag{8}$$

where the longest relaxation time τ_1 is

$$\tau_1 = \frac{\zeta^{bead}}{16 k_B T\, \beta_s^2 \sin^2\left(\frac{\pi}{2N}\right)} \tag{9}$$

and

$$\beta_s^2 = \frac{3}{2N_{K,s}\, b_K^2}; \quad N_{K,s} = \frac{N_K}{N_s}; \quad \langle R^2\rangle_0 = N_K\, b_K^2 \tag{10}$$

$N_s = N - 1$ is the number of springs, N_K is the number of Kuhn steps in the whole chain, b_K is again the Kuhn step length, which for DNA molecules is twice the persistence length, and $\langle R^2\rangle_0$ is the average square of the end-to-end distance. Also, we have

$$\beta_s^2 \equiv \frac{3N_s}{2\langle R^2\rangle_0} \tag{11}$$

(which is unrelated to the dimensionless shear rate $\beta \equiv \dot{\gamma}\tau$) and ζ^{bead} is the bead drag coefficient.

For polystyrene, $\langle R^2\rangle_0$ can be calculated from

$$\langle R^2\rangle_0 = C_\infty n l^2 \tag{12}$$

where C_∞ is the characteristic ratio, n the number of backbone bonds in the polymer molecule, and l the length of a backbone bond. For polystyrene,

$$n = \frac{M}{52}; \quad l = 1.54\ \text{Å}; \quad C_\infty = 9.6 \tag{13}$$

where M is the polymer molecular weight.

For DNA, $\langle R^2\rangle_0$ can be obtained from

$$\langle R^2\rangle_0 = 2 b_K L \tag{14}$$

where L is the contour length of the DNA molecule.

Table 1. Parameters for Polystyrene and DNA Molecules

	λ-phage DNA	3 M PS
L (μm)	21.2	7.285
$b_K = 2A$ (μm)	0.132	0.001803
N	20, 10, 2	
dt (s)	$5 \times 10^{-7}\tau$, for $\dot{\gamma}\tau < 1$	$5 \times 10^{-7}/\dot{\gamma}$, for $\dot{\gamma}\tau > 1$

2.2. Simulation Method. We simulate both polystyrene and λ-phage DNA molecules in steady-state shear flow. The parameters we use in the simulations are listed in Table 1. First we carry out runs in the absence of flow that are long enough to obtain the average equilibrium values of the square of the radius of gyration $\langle R_g^2\rangle_0$, of the square of the end-to-end separation $\langle R^2\rangle_0$, and of the projected length in one direction in Cartesian coordinate $\langle x\rangle_0$. In the simulation of steady shear flow, we time-average the quantities $\boldsymbol{G}$, R_g^2, and x, starting from a time equal to 10 times the molecule's longest relaxation time and continuing for over 100 relaxation times.

We also used various numbers of beads to describe both DNA molecules and polystyrene molecules, as shown in Table 1. For λ-phage DNA, the molecular length per spring, $L/(N-1)$, is only around 1 μm when 20 beads are used. This distance is about 15 times the molecule's persistence length $A = 0.066$ μm. As shown elsewhere(ref 10), when $L/(N-1)$ decreases to 15 or so, the "free hinges" created by the beads increases the molecule's flexibility somewhat. However, it was shown in ref 10 that this effect can be successfully counteracting by artificially increasing A from 0.066 μm to the value $A_{eff} = 0.096$ μm.

An important difference between λ-phage DNA and the polystyrenes considered here is their molecular "extensibility", i.e., the ratio $E \equiv L/\langle R^2\rangle_0^{1/2}$ of the fully extended length (L) of a polymer molecule to its root-mean-square end-to-end distance $\langle R^2\rangle_0^{1/2}$ at equilibrium

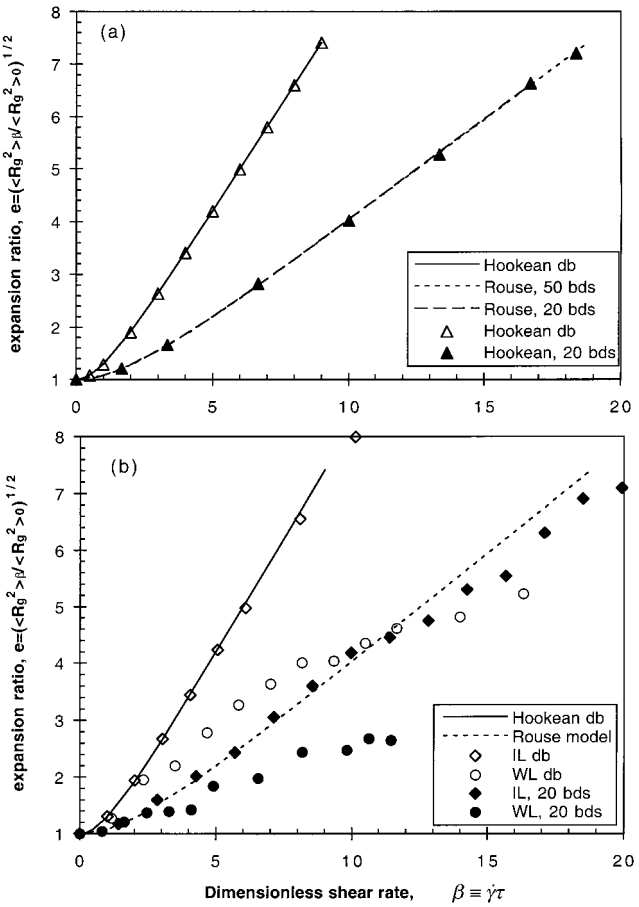

Figure 1. Expansion ratio $e \equiv \langle R_g^2\rangle_\beta^{1/2}/\langle R_g^2\rangle_0^{1/2}$ (a) for infinitely extensible Hookean dumbbell and Rouse models. The lines are from analytic theory, while the symbols are the results from simulations. (b) For a wormlike (WL) chain for λ-phage DNA and an inverse Langevin (IL) chain for polystyrene. In (a) and (b) the lines are from analytic theory for Hookean dumbbell and the Rouse chain; the symbols are simulation results. The solid lines are for an elastic dumbbell, the dashed line is for the Rouse model with 20 beads, and the dotted line is for the Rouse model with 50 beads. The open symbols are for dumbbells, and the solid symbols are for 20-bead chains. The circles are for the wormlike-chain (WL) model of DNA, the diamonds are for the inverse Langevin (IL) model for polystyrene, and in (a) the triangles are for Hookean chains.

(i.e., in the absence of flow). Thus

$$E_{PS} = \frac{L}{\langle R^2\rangle_0^{1/2}} = \frac{0.82nl}{\sqrt{C_\infty nl^2}} = 63.6$$

(polystyrene, $M = 3 \times 10^6$)

$$E_{DNA} = \frac{L}{\langle R^2\rangle_0^{1/2}} = \frac{L}{\sqrt{2AL}} = 12.6$$

(stained λ − phage DNA, $L = 21\ \mu$m)

where $A = 0.066\ \mu$m is the persistence length of the stained DNA molecule. The extensibility of 3 million molecular weight polystyrene is about 5 times larger than that of the λ-phage DNA.

3. Results

First, we compare our simulation results for the expansion ratio e with the analytical solutions from the theories. As shown in Figure 1a, the simulation results for both the Hookean dumbbell (open triangles) and Hookean 20-bead chains (solid triangles) agree well with the analytical solution for the elastic dumbbell (solid line) and the Rouse model (dashed line for 20 beads and dotted line for 50 beads), which was derived by Hoagland and Prud'homme.[17] This figure also shows that there is a big gap between e for the elastic dumbbell model and that for the Rouse model, but the results for 20 beads and 50 beads are almost identical. Figure 1b shows the simulation results for the expansion ratio for λ-phage DNA using a two-bead wormlike (WL) chain (open circles) and a 20-bead wormlike chain (solid circles) and for polystyrene of 3 million molecular weight using the Cohen Padé approximation to the inverse Langevin (IL) function for a two-bead chain (open diamonds) and a 20-bead chain (solid diamonds). The simulation results for 10-bead chains which are not shown in the plots are almost identical to those of 20-bead chains. Compared with the analytical solutions for the elastic dumbbell model (solid line) and the Rouse model (dotted line), the simulation results for the expansion ratio e for DNA (wormlike chain) are much lower than those for the Hookean spring, while the simulated e for polystyrene (inverse Langevin chain) is almost identical to that of the theoretical Hookean spring for β up to about 12, but it falls slightly below the Hookean result for larger β. The reason that e for polystyrene is higher than that for DNA is because of the difference in molecular extensibilities discussed in section 2.

We compare our simulated orientation angle with the predictions of analytic theory in Figure 2a. From the theory,[18] the relationship between the orientation angle χ and the dimensionless shear rate β is

$$\chi = 45° + \frac{\tan^{-1}(\beta/m)}{2} \tag{15}$$

Here m is the "orientation resistance" of the molecule, with $m = 1.0$ for the elastic dumbbell model, $m = 1.75$ for the Rouse model, and $m = 2.553$ for the Zimm model. We can see that the simulation results for the Hookean spring (open triangles for the dumbbell model and solid triangles for the 20-bead model) follow the theoretical results (solid line for elastic dumbbell and dashed line for Rouse model) very well. The results for the inverse Langevin chain model of polystyrene of molecular weight 3 million are about the same as for the Hookean spring, but the results for the wormlike-chain model of λ-phage DNA are lower than the other two. Figure 2b compares experimental light scattering results (symbols) by Lee et al.[7] with the theory (lines). We can see that the experimental results for polystyrene of different molecular weights all fall into the range between Rouse model and Zimm models, although there is no clear trend with molecular weight.

After comparing our simulation results with analytical solutions from theory, we now compare our simulation results for molecular deformation to data from real experimental dilute solutions, one of which is λ-phage DNA studied by Smith et al.[1] and the other is 3 million molecular-weight polystyrene by Lee et al.[7] For DNA, we use a 20-bead model to calculate the mean fractional extension in the flow direction $\langle x/L\rangle$ at various shear rates and plot the results versus dimensionless shear rate $\beta = \dot\gamma\tau$; see Figure 3a. We can see that the simulated results for $\langle x/L\rangle$ (open circles) agree well with the experimental results from Chu's group (for solvent

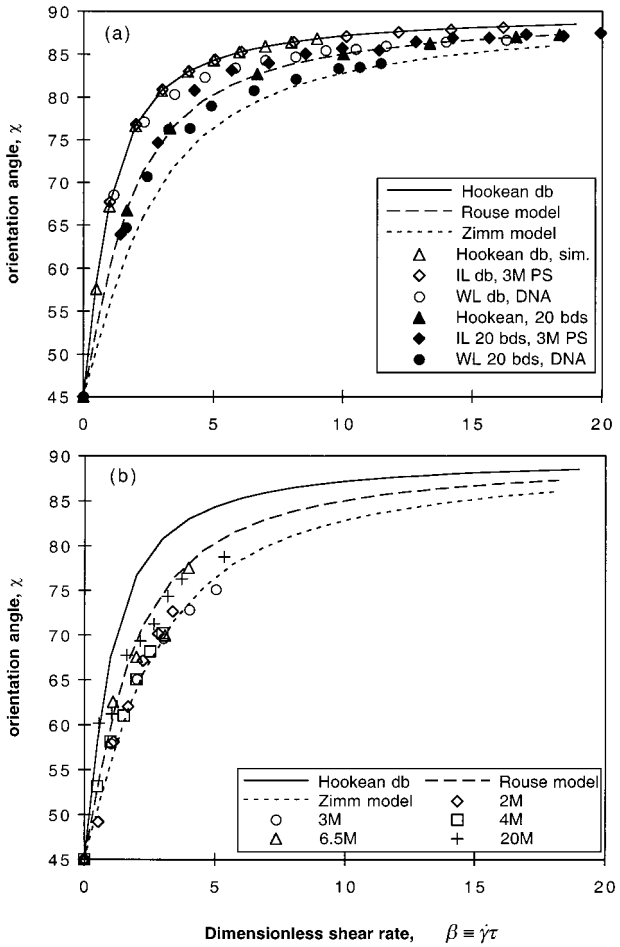

Figure 2. (a) Comparison of the orientation angle χ vs dimensionless shear rate $\beta \equiv \dot{\gamma}\tau$, between theoretical results (lines) and simulation results (symbols). The open symbols are for simulated two-bead (dumbbell) models, and the solid symbols are for simulated 20-bead models. The triangles are for a Hookean chain, the diamonds are for the inverse Langevin-spring model of polystyrene of molecular weight 3 million, and the circles are for the wormlike chain model of DNA. (b) The lines are the same as in (a), while the symbols are experimental data for polystyrenes of molecular weights ranging from 2 to 20 million.

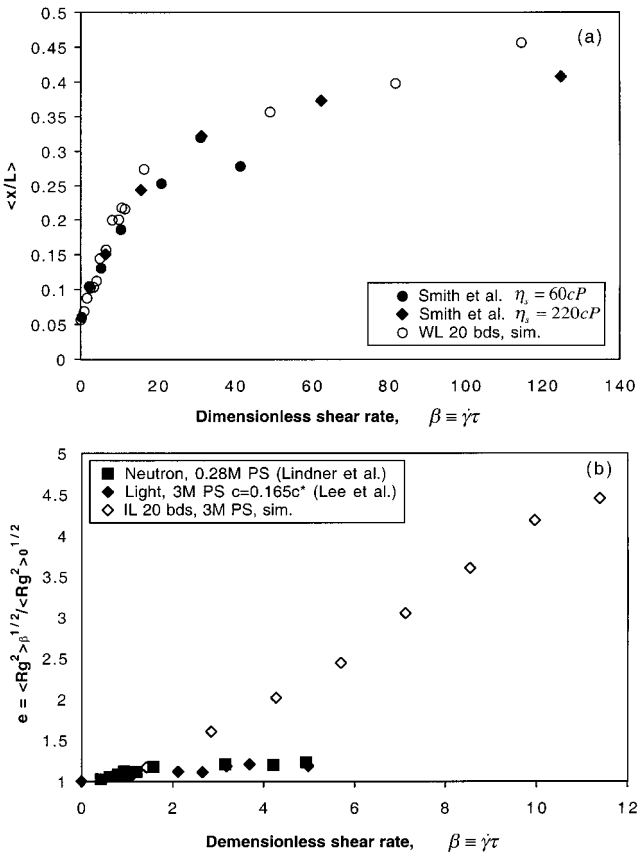

Figure 3. Comparison between experimental results (solid symbols) and simulation results (open symbols) for (a) mean fractional extension in the flow direction for λ-phage DNA and (b) expansion ratio for polystyrene.

viscosity $\eta_s = 60$ cP, solid circles; for $\eta_s = 220$ cP, solid squares).[1] For polystyrene, we also use a 20-bead model to calculate the expansion ratio $e \equiv \langle R_g^2\rangle_\beta^{1/2}/\langle R_g^2\rangle_0^{1/2}$ at various shear rates. Here $\langle R_g^2\rangle_\beta$ is calculated by eq 6 in the presence of shearing flow. The plot of the expansion ratio e vs β in Figure 3b shows that the simulation results (open diamonds) vastly overpredict the experimental data (solid diamonds and solid squares).

The above comparison shows that the simulated mean fractional extension $\langle x/L\rangle$ in the flow direction for DNA agrees well with the experimental observations of individual DNA molecules, while the simulated expansion ratio e for polystyrene deviates greatly from experimental light-scattering and neutron-scattering results.[7,9] In Figure 4 we compare the simulated expansion ratio e for DNA (open circles) with that of polystyrene (open diamonds). As noted earlier, the simulation value of e for polystyrene is higher than that for DNA at each value of β, because of the higher extensibility of the former. Also plotted in Figure 4 are the theoretical predictions of e from the Rouse and Zimm theories for Hookean bead−spring chains.[19] For the Zimm theory, the predictions depend on the value of "hydrodynamic

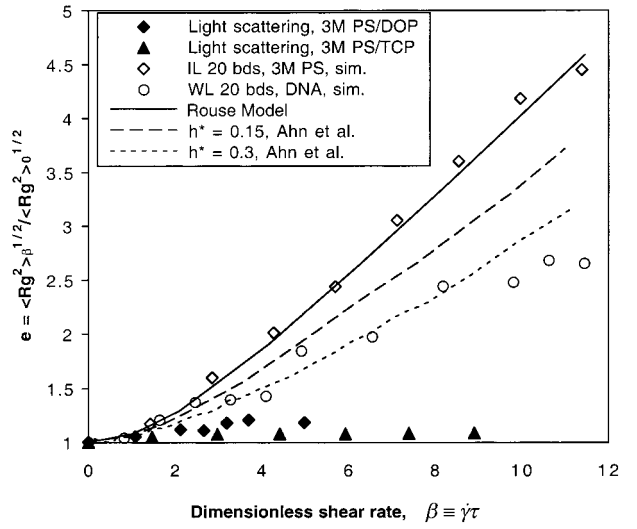

Figure 4. Comparison of expansion ratio from simulations of both DNA (open circles) and polystyrene (open diamonds) with the light-scattering results for polystyrene in DOP solvent (solid diamonds) and in TCP solvent (solid triangles). The lines are theoretical predictions for the Rouse model (solid line), the Zimm model with hydrodynamic interaction parameter $h^* = 0.15$ (dashed line), and for the Zimm model with $h^* = 0.3$ (dotted line).

interaction parameter" h^*. $h^* = 0$ corresponds to the Rouse theory, with no hydrodynamic interaction; increasing h^* implies an increasing level of hydrodynamic interaction, with $h^* = 0.25-0.3$ considered to be maximum value of h^*, appropriate for polystyrene in Θ solvent. Note in Figure 4 that the expansion ratio at

each value of β decreases with increasing h^*. However, even for $h^* = 0.30$, the predicted expansion ratio greatly exceeds that measured by light scattering for polystyrene in various solvents. While the calculations of e from the Zimm theory assume Hookean springs, for polystyrene of molecular weight 3 million the effect of the non-Hookean finitely extensible spring is only significant for $\beta \geq 12$ and so cannot account for the huge deviation between the measured and predicted values of e for $\beta \leq 12$. Also shown in Figure 4 are the light-scattering results for polystyrene of molecular weight 3 million in two different solvents, namely a Θ solvent, DOP (solid diamonds),[7] and a "good" solvent, TCP (solid triangles).[8] The results for both solvents are far below the theoretical predictions (lines).

4. Discussion and Summary

Although measurements of molecular deformation under shear of both λ-phage DNA and polystyrene have been carried out, the molecular "deformation" measured in microscopy experiments with DNA is $\langle x \rangle$, the projected molecular length in the flow direction, which is not directly comparable with the measurement of deformation obtained in light-scattering experiments with polystyrene. In the polystyrene experiments, the measured quantity is the expansion ratio $e \equiv \langle R_g^2 \rangle_\beta^{1/2} / \langle R_g^2 \rangle_0^{1/2}$, the root-mean-square radius of gyration relative to that at equilibrium. Nevertheless, the results of the two experiments can be compared with each other indirectly by comparing both measurements to the results of Brownian dynamics simulations, whose input parameters are suitably chosen to match, in turn, both DNA and polystyrene molecular characteristics. We thereby find excellent agreement between predicted and measured molecular deformation for DNA molecules. We can therefore confidently use the simulations to predict the expansion ratio e for DNA and polystyrene molecules and compare this to the expansion ratio actually measured for polystyrene by light scattering.

Paradoxically, when this is done, we find that although the polystyrene molecules considered here have a greater molecular "stretchability" than that of λ-phage DNA, the light-scattering experiments for polystyrene solutions under shear flow show less stretching at a given strain rate than is obtained for λ-phage DNA under an equivalent shearing flow. A similar conclusion would also surely apply to extensional flows, for which excellent agreement between simulations and DNA experiments is obtained.[10] But for polystyrene solutions, light-scattering studies in extensional flow show that the stretching of the major axis of the radius of gyration tensor never exceeds a factor of 2 even at $\beta \gg 1$.[3,4]

Lacking a convincing explanation for the large difference in the observed deformation of polystyrene molecules relative to that of DNA, we can only note that the possible explanations fall into three categories: (a) differences between DNA and polystyrene molecules, (b) differences between solvent effects in the two cases, and (c) differences in experimental techniques, i.e., direct microscopy versus light scattering.

With respect to the first two categories, we note that DNA has a much larger effective diameter than polystyrene and hence its solvent (water) might behave more like an ideal continuum than is the case with polystyrene. Also, DNA is a polyelectrolyte and hence is a much more expanded coil than is polystyrene. While our simulations are restricted to Θ conditions, experiments with polystyrene in a good solvent (tricresyl phosphate) show even less deformation in light-scattering experiments than is the case with Θ solvent.[8] With regard to category 3, light scattering is a less direct measure of coil size than is video microscopy, and perhaps there exist some undiscovered difficulties in interpreting light-scattering data when coils are strongly deformed by flow.

Acknowledgment. We are grateful for useful discussions with Michael Solomon. Li and Larson were supported under NSF Grant CTS-9707778.

References and Notes

(1) Smith, D. E.; Babcock, H. P.; Chu, S. *Science* **1999**, *283*, 1724.
(2) Armstrong, R. C.; Gupta, S. K.; Basaran, O. *Polym. Eng. Sci.* **1980**, *20*, 466.
(3) Menasveta, M. J.; Hoagland, D. A. *Macromolecules* **1991**, *24*, 3427.
(4) Lee, E. C.; Muller, S. *Macromolecules* **1999**, *32*, 3295.
(5) Cottrell, F. R.; Merrill, E. W.; Smith, K. A. J. *Polym. Sci., Polym. Phys. Ed.* **1969,** *7*, 1415.
(6) Link, A.; Springer, J. *Macromolecules* **1993**, *26*, 464.
(7) Lee, E. C.; Solomon, M.; Muller, S. *Macromolecules* **1997**, *30*, 7313.
(8) Lee, E. C.; Muller, S. *Polymer* **1999**, *40*, 2501.
(9) Lindner, P.; Oberthur, R. *Colloid Polym. Sci.* **1988**, *266*, 886.
(10) Larson, R. G.; Hu, H.; Smith, D. E.; Chu, S. *J. Rheol.* **1999**, *43*, 267.
(11) Hur, J. S.; Larson, R. G.; Shaqfeh, E. S. G., submitted for publication.
(12) Li, L.; Larson, R. G.; Sridhar, T. *J. Rheol.*, in press.
(13) Doyle, P. S.; Shaqfeh, E. S. G.; McKinley, G. H.; Spiegelberg, S. H. *J. Non-Newtonian Fluid Mech.* **1998**, *76*, 79.
(14) Cohen, A. *Rheol. Acta* **1991**, *30*, 270.
(15) Bustamante, C.; Marko, J. F.; Siggia, E. D.; Smith, S. *Science* **1994**, *265*, 1599.
(16) Marko, J. F.; Siggia, E. D. *Macromolecules* **1995**, *28*, 8759.
(17) Hoagland, D. A.; Prudhomme, R. K. *J. Non-Newt. Fluid Mech.* **1988**, *27*, 223.
(18) Peterlin, A. *J. Polym. Sci.* **1957**, *23*, 189.
(19) Ahn, K. H.; Schrag, J. L.; Lee, S. J. *J. Non-Newtonian Fluid Mech.* **1993**, *50*, 349.

MA991090Z